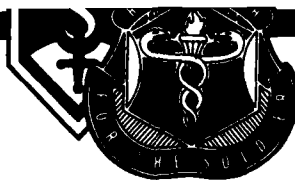# Ultraviolet Radiation Effects on the Corneal Epithelium

DTIC
ELECTE
MAR 1 4 1991
S D
D

By

Morris R. Lattimore

Sensory Research Division

February 1991

91 3 12 060

United States Army Aeromedical Research Laboratory
Fort Rucker, Alabama 36362-5292

Notice

Qualified requesters

Qualified requesters may obtain copies from the Defense Technical Information Center (DTIC), Cameron Station, Alexandria, Virginia 22314. Orders will be expedited if placed through the librarian or other person designated to request documents from DTIC.

Change of address

Organizations receiving reports from the U.S. Army Aeromedical Research Laboratory on automatic mailing lists should confirm correct address when corresponding about laboratory reports.

Animal use

In conducting the research described in this report, the investigators adhered to the Guide for the care and use of laboratory animals, as promulgated by the Committee on Care and Use of Laboratory Animals, National Academy of Sciences-National Research Council.
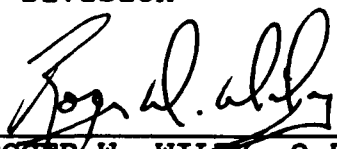
Disposition

Destroy this report when it is no longer needed. Do not return to the originator.

Disclaimer

The views, opinions, and/or findings contained in this report are those of the authors and should not be construed as an official Department of the Army position, policy, or decision unless so designated by other official documentation. Citation of trade names in this report does not constitute an official Department of the Army endorsement or approval of the use of such commercial items.

Reviewed:

THOMAS L. FREZELL
LTC, MS
Director, Sensory Research
  Division

Released for publication:

ROGER W. WILEY, O.D., Ph.D.
Chairman, Scientific
  Review Committee

DAVID H. KARNEY
Colonel, MC, SFS
Commanding

REPORT DOCUMENTATION PAGE		Form Approved OMB No. 0704-0188

1a. REPORT SECURITY CLASSIFICATION	1b RESTRICTIVE MARKINGS
Unclassified	

2a. SECURITY CLASSIFICATION AUTHORITY	3 DISTRIBUTION/AVAILABILITY OF REPORT
	Approved for public release; distribution unlimited
2b. DECLASSIFICATION/DOWNGRADING SCHEDULE	

4. PERFORMING ORGANIZATION REPORT NUMBER(S)	5. MONITORING ORGANIZATION REPORT NUMBER(S)
USAARL Report No. 91-10	

6a. NAME OF PERFORMING ORGANIZATION	6b. OFFICE SYMBOL (If applicable)	7a. NAME OF MONITORING ORGANIZATION
U.S. Army Aeromedical Research Laboratory	SGRD-UAS-VS	U.S. Army Medical Research and Development Command

6c. ADDRESS (City, State, and ZIP Code)	7b. ADDRESS (City, State, and ZIP Code)
Fort Rucker, AL 36362-5292	Fort Detrick Frederick, MD 21702-5012

8a. NAME OF FUNDING/SPONSORING ORGANIZATION	8b. OFFICE SYMBOL (If applicable)	9. PROCUREMENT INSTRUMENT IDENTIFICATION NUMBER

8c. ADDRESS (City, State, and ZIP Code)	10. SOURCE OF FUNDING NUMBERS			
	PROGRAM ELEMENT NO.	PROJECT NO.	TASK NO.	WORK UNIT ACCESSION NO.
	62787A	3M162787A879	BG	168

11. TITLE (Include Security Classification)

Ultraviolet Radiation Effects on the Corneal Epithelium (U)

12. PERSONAL AUTHOR(S)
Morris R. Lattimore

13a. TYPE OF REPORT	13b. TIME COVERED FROM _____ TO _____	14. DATE OF REPORT (Year, Month, Day) 1991 February	15. PAGE COUNT 20

16. SUPPLEMENTARY NOTATION   Presented at the AGARD Aerospace Medical Panel Symposium on Ocular Hazards in Flight and Remedial Measures, 22-26 October 1990, London, UK.

17. COSATI CODES			18. SUBJECT TERMS (Continue on reverse if necessary and identify by block number)
FIELD	GROUP	SUB-GROUP	UVR, corneal epithelium, metabolism, glucose, oxygen
06	04		
20	06		

19. ABSTRACT (Continue on reverse if necessary and identify by block number)

Since military troops are involved in extensive outdoor activities with chronic exposure to solar radiation, and since ultraviolet radiation (UVR) lasers may play a role in the future military environment, a thorough understanding of UVR damage mechanisms would be crucial to the development of intervention and treatment modalities. The present research was directed at quantifying possible alterations in corneal epithelial metabolic activity secondary to in vivo exposure to UVR in the rabbits.

J/cu cm

A 5,000 watt Hg-Xe arc lamp served as the UVR source. The radiant exposures were kept constant at 0.05 $J \cdot cm^{-2}$ for all UVR wavelengths used (290, 300, 310, and 360 nm). Wavelength isolation was accomplished with a double monochromator providing a 6 nm full bandpass. The four experimental wavelengths were chosen based on an interest in maintaining an environmental relevance, since 290 nm UVR and above can be found at the earth's
Continued

20. DISTRIBUTION/AVAILABILITY OF ABSTRACT	21. ABSTRACT SECURITY CLASSIFICATION
☒ UNCLASSIFIED/UNLIMITED ☐ SAME AS RPT. ☐ DTIC USERS	Unclassified

22a. NAME OF RESPONSIBLE INDIVIDUAL	22b. TELEPHONE (Include Area Code)	22c. OFFICE SYMBOL
Chief, Scientific Information Center	(205) 255-6907	SGRD-UAX-SI

DD Form 1473, JUN 86   Previous editions are obsolete.   SECURITY CLASSIFICATION OF THIS PAGE

19. ABSTRACT (Continued)

surface. Micropolarographic measurement of corneal oxygen uptake rates served as an _in vivo_ index of UVR-induced effects on oxidative metabolism. Microfluorometric analyses of key epithelial energy metabolites (glucose, glycogen, ATP, and PCr) were used as an _in vitro_ index of UVR-induced effects on overall metabolic activity. A paired difference analysis of the oxygen uptake rate data demonstrated a decrease in relative corneal oxidative metabolic activity that was wavelength-dependent. These same experimental UVR exposure conditions served to significantly increase epithelial glucose and glycogen concentrations. Although the epithelial ATP concentrations were unchanged, the epithelial PCr concentrations (a

(cont)   high energy phosphate bond reservoir) decreased as a result of UVR exposure.

These data demonstrates a decrease in corneal epithelial oxidative metabolic activity as a result of UVR exposure, and infer an adverse effect on glycolytic metabolism, as well. It is suggested that immediate UVR-induced metabolic inhibitory effects can be responsible for the pattern of epithelial cell loss seen in photokeratitis.

Table of contents

List of figures

1

Accesion For

NTIS CRA&I		☑
DTIC TAB		☐
Unannounced		☐
Justification		

By

Distribution /

Availability Codes

Dist	Avail and/or Special
A-1	

This page intentionally left blank.

Introduction[1]

Ultraviolet radiation (UVR) has been implicated within public health arenas as a potential stimulus for degenerative ocular changes since the time of the ancient Greeks.[2] Recent speculation concerning changes in the nature of the atmospheric ozone layer has led to increased interest in adverse effects of UVR exposure. The advent of UVR lasers have further spurred research interest concerning the determination of possible mechanisms of action, since the development of a full spectrum of applications is dependent upon a thorough understanding of operant mechanisms.

The ideal tissue for investigating the _in vivo_ effects of UVR is the corneal epithelium. As the most anterior tissue layer of the eye, the corneal epithelium is subject to a direct interaction with incident radiation. The tissue is uncomplicated by spurious absorbers, thermal effects, or pigmentary photochemistry. In addition, its avascularity and accessability enable response gathering uninfluenced by circulatory system factors remotely external to the tissue. Finally, the corneal epithelium is exposed to UVR on a daily basis, so exposure studies are not subjecting the tissue to a completely unnatural condition.

Many investigations into the effects of UVR on the corneal epithelium have concentrated on morphological evaluations utilizing the biomicroscope, the light microscope, and/or the electron microscope (Verhoeff and Bell, 1916; Cogan and Kinsey, 1946; Pitts and Tredici, 1971; Ringvold, 1980 and 1983). Such studies have provided detailed information concerning the delayed structural changes characteristic of UVR damage that occur 4 to 12 hours after exposure. As a result of this histological detection delay, information concerning either immediate or functional effects of UVR cannot be probed by such methods.

Millodot and Earlam (1984), seeking to evaluate this damage-delay phenomenon, revealed the presence of a period of decreased corneal sensitivity immediately following exposure to UVR. Their finding appears to signify an immediate effect of UVR upon the sensory neurons subserving the corneal epithelium. If such is the case, and knowing that these axons appear deep within the

---

[1] Presented at the AGARD Aerospace Medical Panel Symposium on Ocular Hazards in Flight and Remedial Measures, 22-26 October, 1990. London, UK.

[2] Xenophan's treatise "Anabasis" discusses the condition of "snowblindness."

basal cell layer of the corneal epithelium and within the anterior stroma, it would be reasonable to assume that there might also be an immediate effect of UVR on the corneal epithelium itself. Therefore, the purpose of this study was to evaluate the possible immediate effect of exposure to UVR on the metabolism of the corneal epithelium in the rabbit.

Selection of the exposure wavelengths (290, 300, 310, and 360 nm) was based on an interest in maintaining an environmental relevance. An additional factor was the intention of creating a distinctive span of effects by maintaining a constant level of radiant exposure at 0.05 $J \cdot cm^{-2}$ with varied wavelength challenges. Measurement of the corneal oxygen uptake rate served as an _in vivo_ assessment of epithelial metabolic activity, while micro-fluorometric metabolite analyses served as an _in vitro_ index of epithelial metabolic activity.

Materials and methods

Experimental animals

Healthy, adult, Dutch-belted, pigmented rabbits were used as the experimental animals. The animals were housed in NIH-approved quarters under controlled, normal lighting conditions. The animals were maintained, and the experiments were conducted in accordance with procedures outlined in the "Guide for Laboratory Animals Facilities and Care" of the National Academy of Sciences-National Research Council. Anesthesia was maintained throughout the course of the experiment with intramuscular injections of Ketalar (10 mg/kg) and Rompun (5 mg/kg). The UVR-exposed animals were sacrificed by cervical dislocation 2 minutes after exposure was discontinued. The eyes were then immediately removed and immersed in liquid nitrogen in order to prevent significant change in metabolite levels. Control animals, after a mock-exposure period under the same level of anesthesia as the experimental animals, underwent the same tissue preparation procedures.

Oxygen electrode

The micropolarographic oxygen probe consisted of a platinum cathode (25-um diameter) and a silver anode embedded in a plastic carrier. A potassium chloride (KCl) solution served as an electrolyte bridge between the cathode and the anode. An oxygen-permeable polyethylene membrane, 25 um thick, effectively sealed the entire electrode-KCl assembly into one operating unit. The micropolarographic system was similar to that used by Benjamin and Hill (1986).

4

In general terms, when a voltage is imposed across the KCl bridge from the anode to the cathode, oxygen present at the sensor tip undergoes an electrolytic reduction at the platinum cathode, with the reverse reaction occuring at the anode. The current generated across the cathode/anode gap is directly proportional to the oxygen concentration of the solution when the system is properly calibrated. The generated current is amplified by a blood gas analyzer and recorded vs time on a physiograph.

Calibration procedure

The probe was calibrated by first placing it in an air-saturated saline solution of 155 mm Hg partial pressure of oxygen. The probe was then placed in a nitrogen-saturated saline solution of 0 mm Hg partial pressure of oxygen. The time required for the recorded oxygen tension to then drop from 140 mm Hg to 40 mm Hg provided the time constant of the micropolarographic system. The experimental procedure involved applying the probe to the anterior surface of the corneal epithelium of the living, anesthetized rabbit. The sensor, when applied to the eye, provided a limited reservoir of oxygen for the underlying tissue. The average rate of oxygen depletion from the sensor reservoir, between recordings of 140 and 40 mm Hg, and after correction for the time constant, became the measure of corneal oxygen uptake rate, which in turn represented a relative measure of the aerobic requirement of the corneal epithelium. Since the aerobic metabolic rate of a tissue directly reflects mitochondrial function (Graymore, 1969), a micropolarographic oxygen electrode, when used to record the rate of oxygen uptake by the anterior surface of the intact cornea, would primarily serve as a relative index of corneal mitochondrial activity.

In vivo micropolarographic application

The eyes of 32 rabbits were exposed in vivo to specific radiant exposure levels of UVR. There were 8 rabbits used in the 290 nm experimental group, 12 rabbits used in the 300 nm experimental group, 7 rabbits used in the 310 nm experimental group, and 5 rabbits used in the 360 nm experimental group. Prior to UVR exposure, five baseline oxygen uptake rates were determined for each eye using a micropolarographic oxygen sensor that was attached to a pH/blood gas monitor in the fashion of Benjamin and Hill (1986). Oxygen uptake rates again were determined 2 minutes post-UVR exposure, enabling the experimenter to compare the change in oxygen uptake rate as a result of the UVR exposure. The uptake rate values were subjected to a paired-difference analysis. A two-way analysis of variance (ANOVA) was performed to examine both within and between experimental groups, and to determine the presence or absence of an overall effect of UVR on the measured oxygen uptake rates.

5

In vitro processing procedure

The rabbit eyes were transferred from the liquid nitrogen container into a -80° C freezer for storage until tissue processing could be accomplished. The cornea was removed from the globe by dissection under -30° C conditions in a wedeen-type cryostat. The isolated cornea was cut into halves, which were mounted on a sectioning button by immersion in a dry ice-cooled hexane solution. The corneal button-mount then was transferred to a cryostatic microtome where tissue sectioning was performed. The resulting central cornea cross sections were approximately 20 micrometers (μm) in thickness. The sectioned tissue samples were placed in a metal tissue holder, covered with glass slides, and inserted into a vacuum tube. The tube was placed in a -20° C freezer and attached to a vacuum pump. The tissue then was freeze-dried for a 24 hour period. After the freeze-drying process was completed the tissue was kept at -20° C until assayed.

Samples needed for assay were thawed under vacuum for 1 hour to prevent condensation-stimulated enzyme action. The different layers of the cornea were defined clearly which permitted easy isolation of the corneal epithelium under a 3X binocular dissecting microscope. Tissue size was determined by dry weight, rather than by tissue section dimensions, which permitted the analysis of very small and irregularly shaped specimens. The tissue samples immediately were weighed on a quartz fiber fishpole balance possessing μg sensitivity. After weighing and recovery, the samples were placed in an oil well rack for specific metabolite assay.

Underlying principles

The cycling system contains several enzymes which catalyze specific interrelated reactions yielding a "net reaction." A byproduct of this multi-step reaction is reduced nicotinamide adenine dinucleotide phosphate (NADPH), which fluoresces light of 460 nm wavelength when excited with UVR of 340 nm wavelength. By measuring the amount of this reduced pyridine nucleotide fluorescence, the original concentration of the assayed metabolite can be inferred by calculation (Lowry and Passonneau, 1972). Appropriate blanks and standards were employed to monitor the reliability of the assays. Individual enzymatic cycling and incubating techniques permitted isolation of the specific metabolite being analyzed.

Source measurement

Source calibration and radiometric quantification followed the procedures described by Pitts, Cullen, and Hacker (1977). The UVR source was a 5,000 watt xenon-mercury (Xe-Hg) high pressure arc lamp, powered by a 10 kilowatt (kw) direct current

power supply regulated to $^+/_-$ 0.5 percent and capable of delivering from 0 to 80 amps at 25 to 65 volts to the arc electrodes. The lamp housing was cooled by a double-blower system. The radiation from the source was focused at a monochromator entrance slit by the housing optics. A 10 cm quartz-enclosed water chamber was placed between the focusing lenses and the monochromator in order to remove infrared radiation. The desired UVR waveband was obtained with a double grating monochromator with gratings blazed at 300 nm and grooved with 1,180 grooves/mm, allowing approximately a 5 nm bandpass. The linear dispersion equated to a value of 0.82 nm/mm. Entrance, intermediate, and exit slits were set to pass a nominal full bandpass of 6.6 nm. The system was aligned with a helium-neon laser and the wavelength counter was calibrated with a mercury source. Exposure durations were set with an electronic shutter controlled by a preset counter. The preset counter allowed exposure durations of any desired length with millisecond accuracy.

The exit optical beam was focused by a quartz lens with a beam size of 1.6 cm by 1.8 cm at the plane of the experimental animal's cornea. A 16-junction thermopile, traceable to a National Bureau of Standards (NBS) standard source, was used to characterize the spectral irradiance of the UVR source. When taking the spectral irradiance readings, the thermopile was placed in the same position relative to the monochromator exit port as the rabbit's cornea was to be situated during UVR exposure. The irradiance (E_e), in watts per square centimeter ($W \cdot cm^{-2}$), incident on the thermopile was determined by the following relationship:

$$E_e = kV_t.$$

The value "k" represents the thermopile calibration constant in microwatts per square centimeter per microvolt ($\mu W \cdot cm^{-2} \cdot \mu V^{-1}$), while the value "$V_t$" represents the average (mean) of three thermopile-voltmeter readings in microvolts (μV). The calibration constant for the thermopile used in this experiment was 5.131 $\mu W \cdot cm^{-2} \cdot \mu V^{-1}$. The radiant exposure (H), in Joules per square centimeter ($J \cdot cm^{-2}$), was calculated by the formula:

$$H = E_e t.$$

The value "t" is simply time in seconds; it should be kept in mind that a Joule is a watt-second. Therefore, for a given irradiance "E_e" the exposure duration "t" can be varied to obtain different values of radiant exposure "H" as desired. Conversely, a radiant exposure can be kept constant, even though wavelength irradiance may differ, by varying the time of exposure. This means of output characterization and source calibration was estimated to have a $^+/_-$ 10 percent accuracy.

The variation of "t" in order to obtain a constant "H", in the context of the wavelengths used in this experiment, creates an outcome that is somewhat dependent upon the validity of the principle of reciprocity (i.e., the biological effects or endpoints are independent of exposure time and irradiance). Corneal effects of a krypton-ion laser, with simultaneous output at 350.7 and 356.4 nm (3:1 ratio), illustrates that the product of threshold intensity and the pulsewidth is a constant; the thresholds for multi-pulse exposures have been shown to be in agreement with those for single-pulse exposures (Zuclich and Connolly, 1976). A similar corneal damage pattern can be elicited from helium-cadmium laser data at 325 nm (Ebbers and Sears, 1975). Based on the literature, it would not be unreasonable to assume that reciprocity holds for all four UVR wavelengths utilized in this experiment.

Results

Introductory data (Figures 1 and 2) have been previously published (Lattimore, 1989a; Lattimore, 1989b), and currently are used as a basis for detailed analyses. Figures 3 and 4 isolate oxygen uptake as a function of corneal epithelial PCr, ATP, glucose, and glycogen concentrations. In the current unit format these data are not easily compared in any fashion other than in a general graphical relationship. Within this general framework there is very close correlation, implying a direct relationship between UVR-altered oxygen uptake rate and certain metabolite changes. ATP was found to be stable across all changes in oxygen uptake associated with UVR exposure ($r = 0.07$). Glucose and glycogen were found to accumulate as a function of UVR-altered oxygen uptake ($r = 0.97$ and 0.98, respectively); PCr depletion also correlated well with changes in UVR-altered oxygen uptake rates ($r = 0.84$).

UVR–Altered Corneal O_2 Uptake Rate: Extrapolated Projection to Baseline
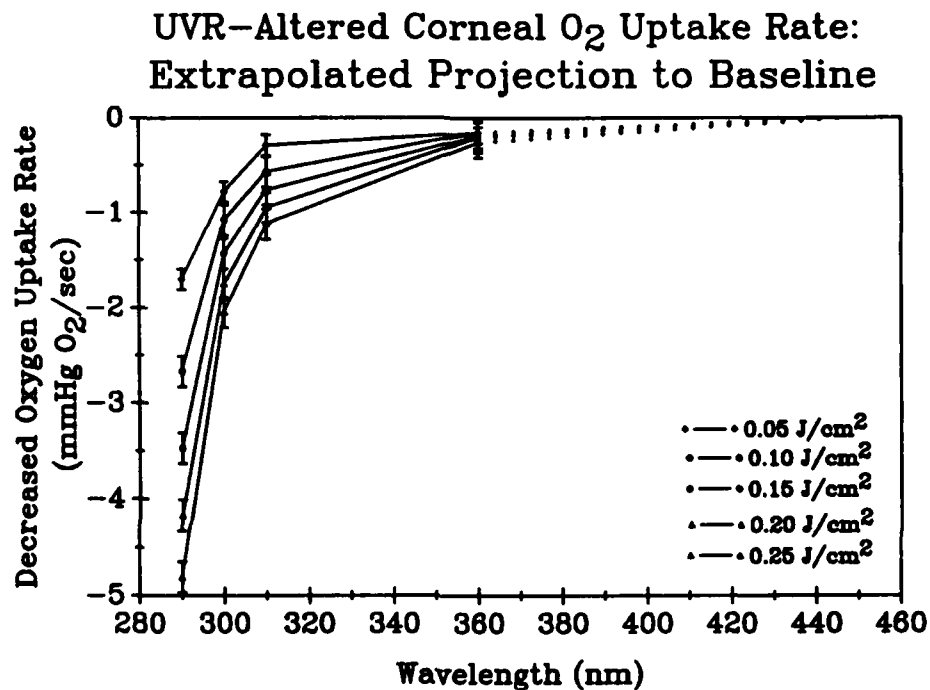
Figure 1 By plotting the UVR-altered corneal oxygen uptake rate data as a function of wavelength, and by making separate datasets for each radiant exposure, a "family" of plots is obtained. A two-way analysis of variance demonstrated an overall significant between-groups difference ($p < 0.0001$), as well as revealed an interactive effect between wavelength and dose ($p < 0.005$). Unexposed eyes exhibited no significant change in corneal oxygen uptake rates over the course of the experiment.

UVR—Alteration of Corneal Epithelial Metabolites
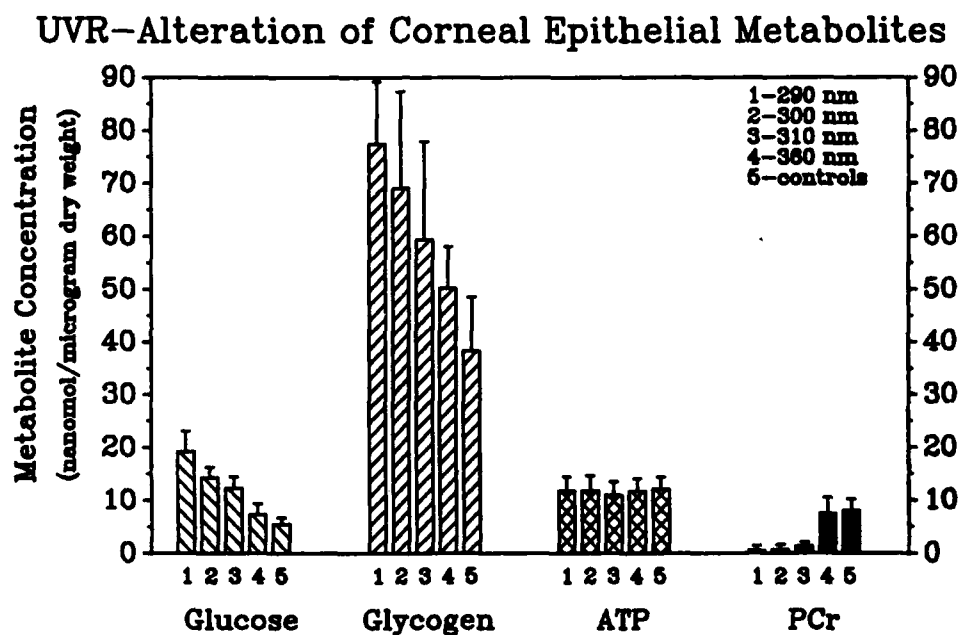
Figure 2   The bar-chart illustrates various epithelial
metabolite concentrations as a function of the
wavelength of UVR exposure. An analysis of variance
of the data demonstrated a highly significant overall,
between groups effect (p<0.0001) for glucose,
glycogen, and PCr. An analysis of variance of ATP
data failed to demonstrate a significant effect
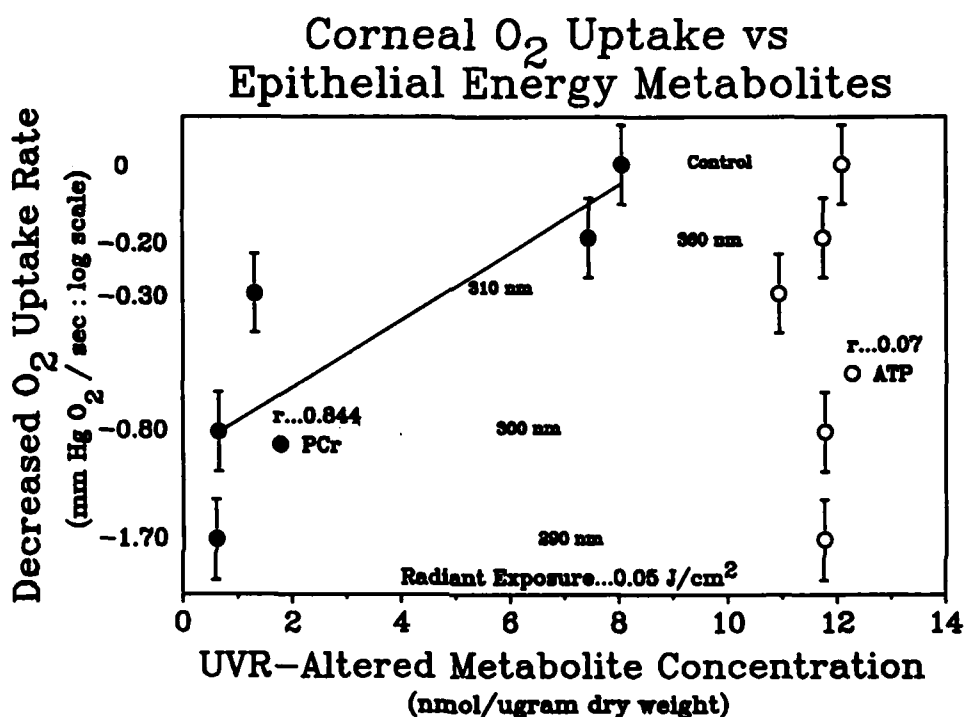(p>0.65), illustrating an apparent ATP-sparing
process.

10

Corneal O$_2$ Uptake vs Epithelial Energy Metabolites

Figure 3   Plotted decreases in the oxygen uptake rate as a function of PCr and ATP, illustrate ATP-sparing at the apparent expense of PCr.

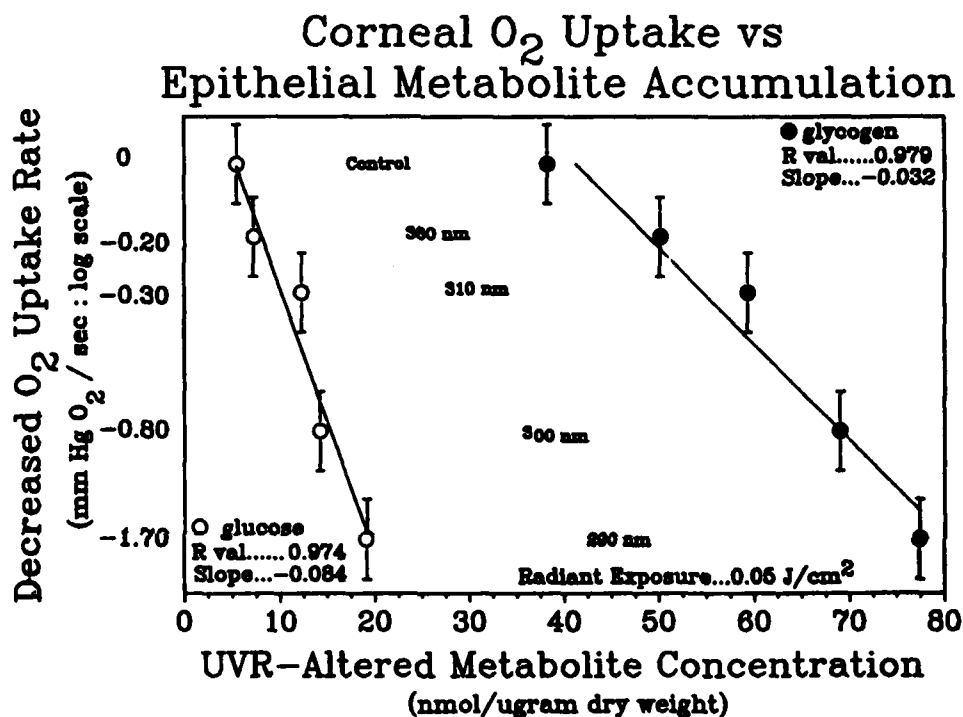## Corneal O$_2$ Uptake vs Epithelial Metabolite Accumulation

Figure 4   Plotted decreases in the oxygen uptake rate correlate highly with accumulations of glucose and glycogen. However, plotted units are not directly mathematically comparable. Therefore, the established relationship between oxygen and glucose should, for the moment, be considered a qualitative relationship only.

Discussion

The corneal epithelium is known to conduct both aerobic and anaerobic metabolic activity concurrently (Kinoshita and Masurat, 1959). According to some estimates, the rabbit corneal epithelium routinely consumes up to 85 percent of available glucose in anaerobic channels, with the remaining 15 percent used via aerobic channels (Riley, 1969). When anaerobic conditions are artificially imposed upon a cornea (i.e., by the application of a thick contact lens), the tissue response has been portrayed to be increased anaerobic activity, inferred by the depletion of epithelial glycogen stores (Uniacke and Hill, 1972). Yet, under the UVR exposure conditions of this experiment, decreased oxygen utilization was evidenced with a contradictory accumulation of both glucose and glycogen, rather than the expected depletion. This paradox led to the examination of oxygen uptake changes as a dependent variable of key metabolites.

The results indicate: a decrease in oxygen consumption, an apparent decrease in glucose utilization, a stabilization of ATP, and a decrement in PCr. The manifested close relationship between the research variables point toward an alteration of oxidative or mitochondrial activity resulting from UVR exposure. In addition, paradoxical glucose and glycogen accumulations suggest a secondary underlying effect on the anaerobic or glycolytic chain. A global enzyme inactivation can be excluded because glycogen and ATP storing are mediated enzymatically. Therefore, it can be concluded that observed UVR effects are the result of more than one damage mechanism. However, this close correlation stems from a superficial view; translation of oxygen data to units more directly comparable could provide a greater insight into operant mechanisms of UVR damage.

By plotting oxygen uptake changes as a function of exposure duration (Figure 5), one can examine slope differences in wavelength effects. The 360 nm data possess a distinctly different slope than the other wavelengths. Since 360 nm oxygen and PCr levels are not significantly affected by UVR exposure, it is likely that 360 nm effects of UVR are not centered upon the mitochondria, but elsewhere in the metabolic chain. However, this analysis does not differentiate relative contributions of mitochondrial and anaerobic effects secondary to 290, 300, and 310 nm exposures. In an attempt to accomplish such a differentiation, oxygen data was mathematically integrated over the 0.05 J/cm^2 radiant exposure period. It was not necessary to do this for metabolite data, because metabolite data represent a natural integration over the total exposure.

13

Altered O₂ Uptake vs Exposure Duration
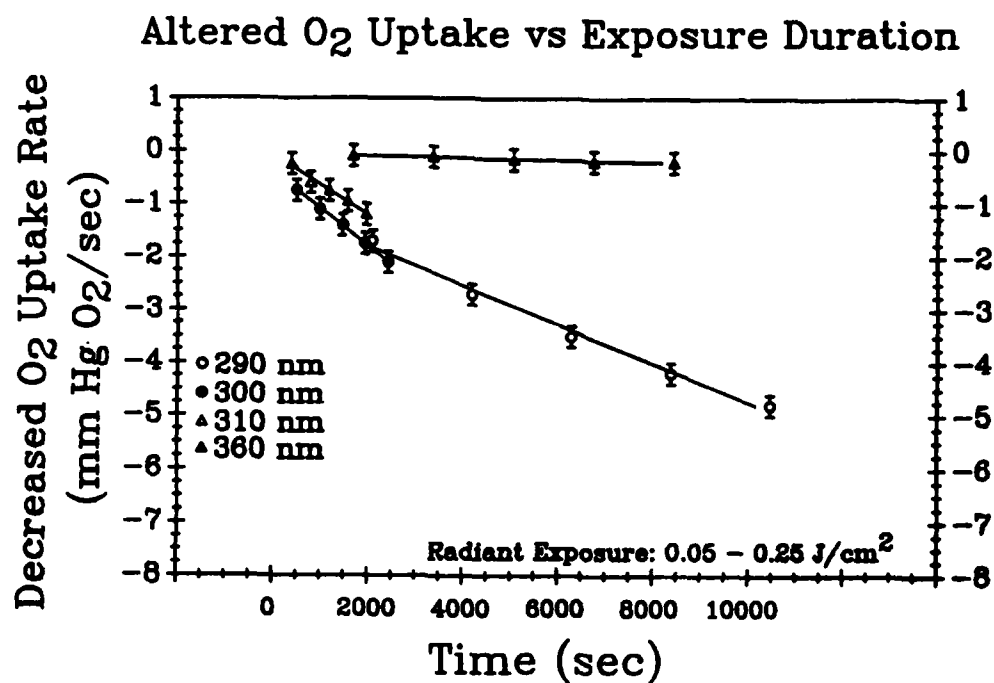
Figure 5   Comparison of the oxygen-exposure time slope data
highlight 360 nm effects to be independent of other
wavelength mechanisms of action.   The combined absence
of oxygen effects accompanied by glucose accumulation
suggest the presence of a damage mechanism isolated
within the anaerobic stages of metabolism.

14

Since oxygen data are theoretically translatable from mm Hg O_2/sec to ul/cm^2, and metabolite data can be translated from nmol/ug to nmol/cm^2, a directly comparable unit correlation may be obtained. This method of data presentation (Figure 6) highlights the relative relationships between mitochondrial and anaerobic metabolism, with UVR wavelength. Short wavelength UVR (i.e., 290 nm and possibly shorter) are shown to possess predominantly an adverse mitochondrial effect on the corneal epithelium, since PCr dramatically falls off compared to the other wavelength exposures, and total glucose accumulations are much less than a standard, linear model would predict. As the exposure wavelength increases, total glucose accumulation and PCr depletion conform to a linear representation when compared to equivalent oxygen decrements. Therefore, it can be concluded that observed UVR effects on the corneal epithelium are the result of more than one damage mechanism. UVR exposures at or near 360 nm will produce effects predominantly by way of disruption of anaerobic/glycolytic metabolic pathways. UVR exposures at and possibly below 290 nm will produce effects predominantly by way of disruption of aerobic/mitochondrial metabolic pathways. UVR exposures at intermediate wavelengths will produce compound effects on the corneal epithelium involving both damage mechanisms.

Summary

Corneal epithelial metabolism is affected adversely by a dual mechanism of UVR damage. This duality differentially presents itself dependent upon exposure wavelength. While considerable overlap is possible, clearly short wavelength UVR is predominantly toxic to the mitochondrial system, while longer wavelength UVR predominantly affects the anaerobic metabolic pathways. Dual damage mechanisms, with overlapping action spectra could complicate the development of intervention and treatment modalities. Specific enzymatic analyses will be necessary to fully elicit wavelength specificities and potential treatment options.

15

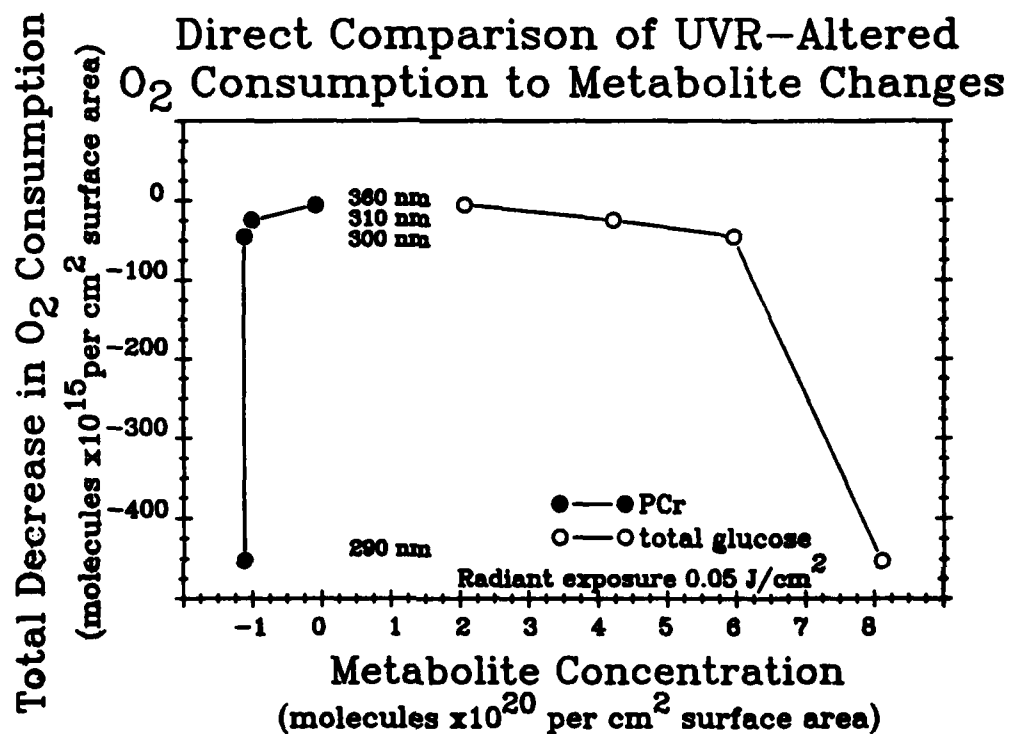Direct Comparison of UVR–Altered O_2 Consumption to Metabolite Changes

Figure 6   Total glucose and PCr concentrations for 290 nm exposures are clearly outside any potential linear relationship that might be suggested by 300, 310, and 360 nm data. This dramatic dropoff in PCr, combined with the nonlinear accumulation of glucose found in 290 nm exposures suggest the presence of a damage mechanism isolated at the level of mitochondrial function.

16

References

Benjamin, W. J., and Hill, R. M. 1986. Human corneal
oxygen demand: the closed eye interval. <u>Graefes archives
of clinical and experimental ophthalmology</u>.
224(3):291-294.

Cogan, D. G., and Kinsey, V. E. 1946. Action spectrum of
keratitis produced by ultraviolet radiation.
<u>Archives of ophthalmology</u>. **35**:670-677.

Ebbers, R. W., and Sears, D. 1975. Ocular effects of a 325
nm ultraviolet laser. <u>American journal of optometry and
physiological optics</u>. **52**:216-219.

Graymore, C. N. 1969. "Biochemistry of the eye." Academic
Press. London, New York.

Kinoshita, J. H., and Masurat, A. B. 1959. Aerobic
pathways of glucose metabolism in bovine corneal
epithelium. <u>American journal of ophthalmology</u>.
48:47-52.

Lattimore, M. R. 1989a. Effects of ultraviolet radiation
on the oxygen uptake rate of the rabbit cornea.
<u>Optometry and vision science</u> **66**:117-122.

Lattimore, M. R. 1989b. Effect of ultraviolet radiation on
the energy metabolism of the corneal epithelium of the
rabbit. <u>Photochemistry and photobiology</u>. **49**:175-180.

Lowry, O. H., and Passonneau, J. V. 1972. "A flexible
system of enzymatic analysis." Academic Press, New York.

Millodot, M., and Earlam, R. A. 1984. Sensitivity of the
cornea after exposure to ultraviolet light. <u>Ophthalmic
research</u>. **16**:325-328.

Pitts, D. G., and Tredici, T. J. 1971. The effects of
ultraviolet on the eye. <u>American industrial hygiene
association journal</u>. **32**:235-246.

Pitts, D. G., Cullen, A. P., and Hacker, P. D. 1977.
Ocular effects of ultraviolet radiation from 295 to
365 nm. <u>Investigative ophthalmology and visual science</u>.
16:932-939.

Riley, M. V. 1969. Glucose and oxygen utilization by the rabbit cornea. Experimental eye research 8:193-197.

Ringvold, A. 1980. Cornea and ultraviolet radiation. Acta ophthalmologica. 58:63-68.

Ringvold, A. 1983. Damage of the corneal epithelium caused by ultraviolet radiation. Acta ophthalmologica. 61:898-907.

Uniacke, C. A., and Hill, R. M. 1972. The depletion course of epithelial glycogen with corneal anoxia. Archives of ophthalmology. 87:56-59.

Verhoeff, F. H., and Bell, L. 1916. The pathological effects of radiant energy on the eye. Proceedings of the American academy of arts and sciences. 61:630-818.

Zuclich, J. A., and Connolly, J. S. 1976. Ocular damage induced by near-ultraviolet laser radiation. Investigative ophthalmology and visual science. 15:760-764.

Initial distribution

Commander, U.S. Army Natick Research,
Development and Evaluation Center
ATTN: STRNC-MIL (Documents
Librarian)
Natick, MA 01760-5040

Naval Submarine Medical
Research Laboratory
Medical Library, Naval Sub Base
Box 900
Groton, CT 06340

Commander/Director
U.S. Army Combat Surveillance
and Target Acquisition Lab
ATTN: DELCS-D
Fort Monmouth, NJ 07703-5304

Commander
10th Medical Laboratory
ATTN: Audiologist
APO New York 09180

Naval Air Development Center
Technical Information Division
Technical Support Detachment
Warminster, PA 18974

Commanding Officer, Naval Medical
Research and Development Command
National Naval Medical Center
Bethesda, MD 20814-5044

Deputy Director, Defense Research
and Engineering
ATTN: Military Assistant
for Medical and Life Sciences
Washington, DC 20301-3080

Commander, U.S. Army Research
Institute of Environmental Medicine
Natick, MA 01760

U.S. Army Avionics Research
and Development Activity
ATTN: SAVAA-P-TP
Fort Monmouth, NJ 07703-5401

U.S. Army Communications-Electronics
Command
ATTN: AMSEL-RD-ESA-D
Fort Monmouth, NJ 07703

Library
Naval Submarine Medical Research Lab
Box 900, Naval Sub Base
Groton, CT 06349-5900

Commander
Man-Machine Integration System
Code 602
Naval Air Development Center
Warminster, PA 18974

Commander
Naval Air Development Center
ATTN: Code 602-B (Mr. Brindle)
Warminster, PA 18974

Commanding Officer
Harry G. Armstrong Aerospace
Medical Research Laboratory
Wright-Patterson
Air Force Base, OH 45433

Director
Army Audiology and Speech Center
Walter Reed Army Medical Center
Washington, DC 20307-5001

Commander, U.S. Army Institute
of Dental Research
ATTN: Jean A. Setterstrom, Ph. D.
Walter Reed Army Medical Center
Washington, DC 20307-5300

Naval Air Systems Command
Technical Air Library 950D
Room 278, Jefferson Plaza II
Department of the Navy
Washington, DC 20361

Naval Research Laboratory Library
Shock and Vibration
  Information Center, Code 5804
Washington, DC 20375

Director, U.S. Army Human
  Engineering Laboratory
ATTN: Technical Library
Aberdeen Proving Ground, MD 21005

Commander, U.S. Army Test
  and Evaluation Command
ATTN: AMSTE-AD-H
Aberdeen Proving Ground, MD 21005

Director
U.S. Army Ballistic
  Research Laboratory
ATTN: DRXBR-OD-ST Tech Reports
Aberdeen Proving Ground, MD 21005

Commander
U.S. Army Medical Research
  Institute of Chemical Defense
ATTN: SGRD-UV-AO
Aberdeen Proving Ground,
MD 21010-5425

Commander, U.S. Army Medical
Research and Development Command
ATTN: SGRD-RMS (Ms. Madigan)
Fort Detrick, Frederick, MD 21702-5012

Director
Walter Reed Army Institute of Research
Washington, DC 20307-5100

HQ DA (DASG-PSP-O)
5109 Leesburg Pike
Falls Church, VA 22041-3258

Naval Research Laboratory
Library Code 1433
Washington, DC 20375

Harry Diamond Laboratories
ATTN: Technical Information Branch
2800 Powder Mill Road
Adelphi, MD 20783-1197

U.S. Army Materiel Systems
  Analysis Agency
ATTN: AMXSY-PA (Reports Processing)
Aberdeen Proving Ground
MD 21005-5071

U.S. Army Ordnance Center
  and School Library
Simpson Hall, Building 3071
Aberdeen Proving Ground, MD 21005

U.S. Army Environmental
  Hygiene Agency
Building E2100
Aberdeen Proving Ground, MD 21010

Technical Library Chemical Research
  and Development Center
Aberdeen   Proving   Ground,   MD
21010--5423

Commander
U.S. Army Medical Research
  Institute of Infectious Disease
SGRD-UIZ-C
Fort Detrick, Frederick, MD 21702

Director, Biological
  Sciences Division
Office of Naval Research
600 North Quincy Street
Arlington, VA 22217

Commander
U.S. Army Materiel Command
ATTN: AMCDE-XS
5001 Eisenhower Avenue
Alexandria, VA 22333

Commandant
U.S. Army Aviation
  Logistics School ATTN: ATSQ-TDN
Fort Eustis, VA 23604

Headquarters (ATMD)
U.S. Army Training
  and Doctrine Command
Fort Monroe, VA 23651

Structures Laboratory Library
USARTL-AVSCOM
NASA Langley Research Center
Mail Stop 266
Hampton, VA 23665

Naval Aerospace Medical
  Institute Library
Building 1953, Code 03L
Pensacola, FL 32508-5600

Command Surgeon
HQ USCENTCOM (CCSG)
U.S. Central Command
MacDill Air Force Base FL 33608

Air University Library
(AUL/LSE)
Maxwell Air Fore Base, AL 36112

U.S. Air Force Institute
  of Technology (AFIT/LDEE)
Building 640, Area B
Wright-Patterson
Air Force Base, OH 45433

Henry L. Taylor
Director, Institute of Aviation
University of Illinois-Willard Airport
Savoy, IL 61874

Chief, Nation Guard Bureau
ATTN: NGB-ARS (COL Urbauer)
Room 410, Park Center 4
4501 Ford Avenue
Alexandria, VA 22302-1451

Commander
U.S. Army Aviation Systems Command
ATTN: SGRD-UAX-AL (MAJ Gillette)
4300 Goodfellow Blvd., Building 105
St. Louis, MO 63120

U.S. Army Aviation Systems Command
Library and Information Center Branch
ATTN: AMSAV-DIL
4300 Goodfellow Boulevard
St. Louis, MO 63120

Federal Aviation Administration
Civil Aeromedical Institute
Library AAM-400A
P.O. Box 25082
Oklahoma City, OK 73125

Commander
U.S. Army Academy
  of Health Sciences
ATTN: Library
Fort Sam Houston, TX 78234

Commander
U.S. Army Institute of Surgical Research
ATTN: SGRD-USM (Jan Duke)
Fort Sam Houston, TX 78234-6200

AAMRL/HEX
Wright-Patterson
Air Force Base, OH 45433

University of Michigan
NASA Center of Excellence in Man-
Systems Research
ATTN: R. G. Snyder, Director
Ann Arbor, MI 48109

John A. Dellinger,
Southwest Research Institute
P. 0. Box 28510
San Antonio, TX 78284

Product Manager
Aviation Life Support Equipment
ATTN: AMCPM-ALSE
4300 Goodfellow Boulevard
St. Louis, MO 63120-1798

Commander
U.S. Army Aviation
    Systems Command
ATTN: AMSAV-ED
4300 Goodfellow Boulevard
St. Louis, MO 63120

Commanding Officer
Naval Biodynamics Laboratory
P.O. Box 24907
New Orleans, LA 70189-0407

Assistant Commandant
U.S. Army Field Artillery School
ATTN: Morris Swott Technical Library
Fort Sill, OK 73503-0312

Commander
U.S. Army Health Services Command
ATTN: HSOP-SO
Fort Sam Houston, TX 78234-6000

Director of Professional Services
HQ USAF/SGDT
Bolling Air Force Base, DC 20332-6188

U.S. Army Dugway Proving Ground
Technical Library, Building 5330
Dugway, UT 84022

U.S. Army Yuma Proving Ground
Technical Library
Yuma, AZ 85364

AFFTC Technical Library
6510 TW/TSTL
Edwards Air Force Base,
CA 93523-5000

Commander
Code 3431
Naval Weapons Center
China Lake, CA 93555

Aeromechanics Laboratory
U.S. Army Research and Technical Labs
Ames Research Center, M/S 215-1
Moffett Field, CA 94035

Sixth U.S. Army
ATTN: SMA
Presidio of San Francisco, CA 94129

Commander
U.S. Army Aeromedical Center
Fort Rucker, AL 36362

U.S. Air Force School
    of Aerospace Medicine
Strughold Aeromedical Library Technical
Reports Section (TSKD)
Brooks Air Force Base, TX 78235-5301

Dr. Diane Damos
Department of Human Factors
ISSM, USC
Los Angeles, CA 90089-0021

U.S. Army White Sands
    Missile Range
ATTN: STEWS-IM-ST
White Sands Missile Range, NM 88002

U.S. Army Aviation Engineering
    Flight Activity
ATTN: SAVTE-M (Tech Lib) Stop 217
Edwards Air Force Base, CA 93523-5000

Ms. Sandra G. Hart
Ames Research Center
MS 262-3
Moffett Field, CA 94035

Commander, Letterman Army Institute
of Research
ATTN: Medical Research Library
Presidio of San Francisco, CA 94129

Mr. Frank J. Stagnaro, ME
Rush Franklin Publishing
300 Orchard City Drive
Campbell, CA 95008

Commander
U.S. Army Medical Materiel
Development Activity
Fort Detrick, Frederick, MD 21702-5009

Commander
U.S. Army Aviation Center
Directorate of Combat Developments
Building 507
Fort Rucker, AL 36362

U. S. Army Research Institute
Aviation R&D Activity
ATTN: PERI-IR
Fort Rucker, AL 36362

Commander
U.S. Army Safety Center
Fort Rucker, AL 36362

U.S. Army Aircraft Development
Test Activity
ATTN: STEBG-MP-P
Cairns Army Air Field
Fort Rucker, AL 36362

Commander U.S. Army Medical Research
and Development Command
ATTN: SGRD-PLC (COL Sedge)
Fort Detrick, Frederick, MD 21702

MAJ John Wilson
TRADOC Aviation LO
Embassy of the United States
APO New York 09777

Netherlands Army Liaison Office
Building 602
Fort Rucker, AL 36362

British Army Liaison Office
Building 602
Fort Rucker, AL 36362

Italian Army Liaison Office
Building 602
Fort Rucker, AL 36362

Directorate of Training Development
Building 502
Fort Rucker, AL 36362

Chief
USAHEL/USAAVNC Field Office
P. O. Box 716
Fort Rucker, AL 36362-5349

Commander U.S. Army Aviation Center
and Fort Rucker
ATTN: ATZQ-CG
Fort Rucker, AL 36362

Commander/President
TEXCOM Aviation Board
Cairns Army Air Field
Fort Rucker, AL 36362

Dr. William E. McLean
Human Engineering Laboratory
ATTN: SLCHE-BR
Aberdeen Proving Ground,
MD 21005-5001

Canadian Army Liaison Office
Building 602
Fort Rucker, AL 36362

German Army Liaison Office
Building 602
Fort Rucker, AL 36362

LTC Patrick Laparra
French Army Liaison Office
USAAVNC (Building 602)
Fort Rucker, AL 36362-5021

Australian Army Liaison Office
Building 602
Fort Rucker, AL 36362

Dr. Garrison Rapmund
6 Burning Tree Court
Bethesda, MD 20817

Commandant Royal Air Force
Institute of Aviation Medicine
Farnborough Hampshire GU14 65Z UK

Dr. A. Kornfield, President
Biosearch Company
3016 Revere Road
Drexel Hill, PA 29026

Commander
U.S. Army Biomedical Research
  and Development Laboratory
ATTN: SGRD-UBZ-I
Fort Detrick, Frederick, MD 21702

Defense Technical Information Center
Cameron Station
Alexandra, VA 22313

Commander, U.S. Army Foreign Science
  and Technology Center
AIFRTA (Davis)
220 7th Street, NE
Charlottesville, VA 22901-5396

Director,
Applied Technology Laboratory
USARTL-AVSCOM
ATTN: Library, Building 401
Fort Eustis, VA 23604

U.S. Army Training
  and Doctrine Command
ATTN: Surgeon
Fort Monroe, VA 23651-5000

Aviation Medicine Clinic
TMC #22, SAAF
Fort Bragg, NC 28305

U.S. Air Force Armament
  Development and Test Center
Eglin Air Force Base, FL 32542

Commander, U.S. Army Missile
Command
Redstone Scientific Information Center
ATTN: AMSMI-RD-CS-R/ILL
Documents Redstone Arsenal, AL 35898

U.S. Army Research and Technology
  Laboratories (AVSCOM)
Propulsion Laboratory MS 302-2
NASA Lewis Research Center
Cleveland, OH 44135

Dr. H. Dix Christensen
Bio-Medical Science Building, Room 753
Post Office Box 26901
Oklahoma City, OK 73190

Col. Otto Schramm Filho
c/o Brazilian Army Commission
  Office-CEBW
4632 Wisconsin Avenue NW
Washington, DC 20016

Dr. Christine Schlichting
Behavioral Sciences Department
Box 900, NAVUBASE NLON
Groton, CT 06349-5900

COL Eugene S. Channing, O.D.
Brooke Army Medical Center
ATTN: HSHE-EAH-O
Fort Sam Houston, TX 78234-6200